

## Emission times for energy selected $^{1,2,3}\text{H}$ ejectiles from central collisions: 1360 MeV $^{40}\text{Ar} + \text{Ag}$

C. J. Gelderloos,<sup>1,\*</sup> Rulin Sun,<sup>1</sup> N. N. Ajitanand,<sup>1</sup> John M. Alexander,<sup>1</sup> E. Bauge,<sup>1,2,†</sup> A. Elmaani,<sup>1,‡</sup> T. Ethvignot,<sup>1,2,†</sup> Roy A. Lacey,<sup>1</sup> M. E. Brandan,<sup>2,§</sup> A. Giorni,<sup>2</sup> D. Heuer,<sup>2</sup> S. Kox,<sup>2</sup> A. Lleres,<sup>2</sup> A. Menchaca-Rocha,<sup>2,§</sup> F. Merchez,<sup>2</sup> D. Rebreyend,<sup>2</sup> J. B. Viano,<sup>2</sup> B. Chambon,<sup>3</sup> B. Cheynis,<sup>3</sup> D. Drain,<sup>3</sup> and C. Pastor<sup>3</sup>

<sup>1</sup>*Departments of Physics and Chemistry, State University of New York at Stony Brook, Stony Brook, New York 11794*

<sup>2</sup>*Institut des Sciences Nucléaires de Grenoble, Institut National de Physique Nucléaire et de Physique des Particules—Centre Nationale de la Recherche Scientifique/Université Joseph Fourier, 53 Avenue des Martyrs, 38026, Grenoble Cedex, France*

<sup>3</sup>*Institut de Physique Nucléaire de Lyon, Institut National de Physique des Particules—Centre National de la Recherche Scientifique/Université Claude Bernard, 43, Blvd. du 11 Novembre 1918, 69622 Villeurbanne, Cedex, France*

(Received 30 March 1995)

For central collisions of 1360 MeV  $^{40}\text{Ar} + \text{Ag}$  we report correlations in relative momentum and in velocity difference for  $^{1,2,3}\text{H}$  ejectiles at  $32^\circ$  and  $68^\circ$ . Comparison to trajectory calculations gives a measure of the mean emission times, and, for unlike pairs, the average emission orders. There is a strong variation of the average emission times as a function of ejectile energy that is very similar for each H isotope; they change from  $\geq 1000$  fm/c for  $\sim 10$  MeV in the c.m. to  $\leq 50$  fm/c for  $\geq 30$  MeV. This indicates a broad spectrum of emission sources and associated characteristics. The longer times suggest evaporative emission from thermalized systems for  $^{1,2,3}\text{H}$  of energies  $\sim 10$  MeV (i.e., those near the emission barrier). The shorter times, along with the observed energy spectra, suggest extensive prethermalization or direct emission from the central collision zone for  $^{1,2,3}\text{H}$  ejectiles of much higher energy.

PACS number(s): 25.70.Pq

Heavy ion induced nuclear reactions give effective pathways for massive energy dissipation into very highly excited central collision zones. For 34A MeV  $^{40}\text{Ar} + \text{Ag}$ , measurements of energy spectra and angular distributions for light charged particles LCP ( $^{1,2,3}\text{H}$  and  $^4\text{He}$ ) at polar angle  $\theta \geq 68^\circ$  show extensive energy thermalization typical of a single heavy emission source [1,2]. For LCP's emitted at  $\theta \leq 68^\circ$ , there is a prominent forward peak in the angular distributions, especially for higher energy particles. This high-energy, forward-peaked LCP emission is often attributed to "projectilelike" and "intermediate-rapidity" sources but, of course, it may also include direct or prethermalization emission. In this paper we present particle-particle correlations measured at both  $\theta_{\text{lab}} \sim 68^\circ$  and  $\sim 32^\circ$ ; the larger angle strongly emphasizes emission after extensive thermalization while the smaller angle emphasizes prethermalization emission. These correlations are analyzed to give mean lifetimes  $\tau$ , [3,4] which are of great interest since they are intimately related to the nature and extent of equilibration. Cuts are made on the ejectile energies  $E_i$  to provide a systematic pattern of  $\tau$  versus  $E_i$  for each of the H isotopes. A particularly simple and dramatic picture emerges for these empirical lifetimes from  $\geq 1000$  fm/c (i.e., characteristic of evaporation) to  $\leq 50$  fm/c (i.e., characteristic of traversal times).

Experimental measurements were made of small-angle ejectile pair correlations with the EMRIC 25-detector array at Grenoble [5] using techniques very similar to [6]. Previous work with a  $4\pi$  multidetector has established that the detection of such a pair in itself selects the central collision group for this reaction [7,8]. Two-particle coincidence events were recorded and used in two ways. Following the usual practice [6] they were binned in relative momentum  $P_{\text{rel}}$  to form a spectrum  $A(P_{\text{rel}})$ . A correlation function is defined as the ratio  $A(P_{\text{rel}})/B(P_{\text{rel}})$  where  $B(P_{\text{rel}})$  is a reference spectrum for the same class of particles but from separate events. We have used event mixing for the construction of the reference spectrum  $B(P_{\text{rel}})$ ; this reference spectrum is area normalized to the total number of events in the real spectrum  $A(P_{\text{rel}})$ . In addition we present velocity difference ( $V_p - V_d$ ) spectra between protons and deuterons recorded for opening angle  $\gamma < 7^\circ$ . The velocity difference spectra are sensitive to the ejectile emission order [4,7,9] as well as the mean lifetime. Trajectory calculations from the reaction simulation code MENEKA [3] are used to interpret both the correlation functions and the velocity difference spectra. These simulations include a detection filter and event processing that duplicate experimental conditions [6].

Figure 1 shows experimental results and reaction simulation calculations for  $^2\text{H}-^2\text{H}$  pairs from the EMRIC array centered at  $\theta = 68^\circ$ . Each velocity difference spectrum on the right utilizes only those coincident pairs recorded in detectors with center-point opening angle  $\gamma < 7^\circ$  (i.e., the nearest and next-nearest neighbors) and energy ranges for individual deuterons as indicated. The associated correlation function on the left involves the same energy cuts for each particle, but all detector pairs are accepted with no selection on  $\gamma$ . Reaction simulation calculations are shown by the various smooth curves and associated mean lifetime values.

\*Present address: Department of Physics, University of Colorado, Boulder, CO 80309-0446.

†Permanent address: Battelle Memorial Institute, 505 King Avenue, Columbus, OH 43201.

‡Permanent address: Centre d'Etudes de Bruyères-Le-Chatel, Service de Physique et Techniques Nucléaires, Boîte Postale No. 12, 91680 Bruyères-Le-Chatel, France.

§Permanent address: Inst. de Fisica UNAM, A.P. 20-364, Mexico-1000 DF, Mexico.

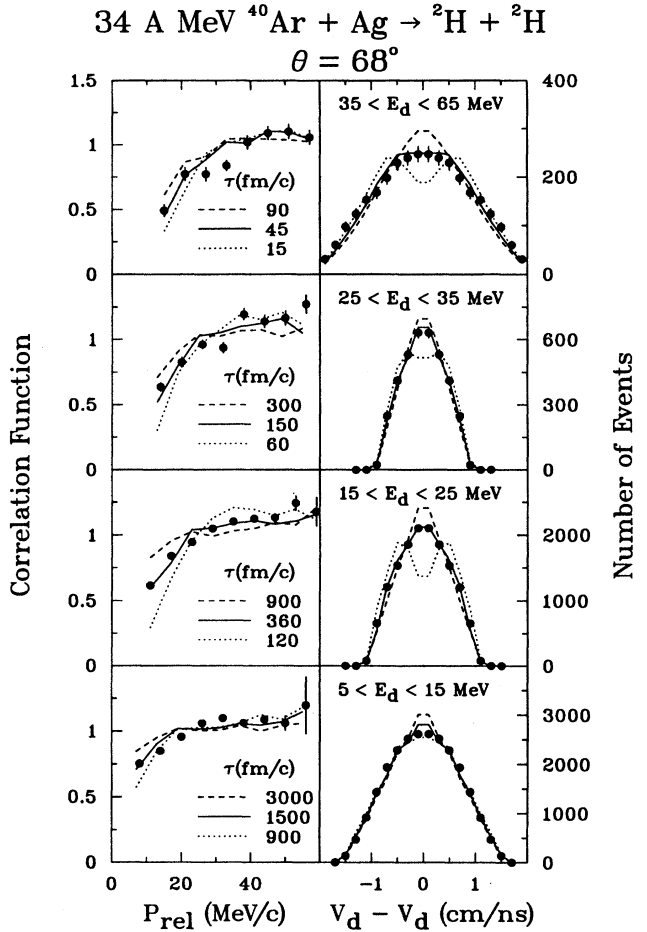


FIG. 1. Correlation functions in relative momentum  $P_{\text{rel}}$  (left) and velocity difference ( $V_d - V_d$ ) spectra (right) for deuteron pairs detected in EMRIC centered at  $68^\circ$ . Energy gates for associated plots are indicated on the right and the mean lifetime (or  $\tau$ ) values used for the calculated curves are indicated on the left. All pairs are included for the correlation functions but only those with  $\gamma < 7^\circ$  for the velocity differences.

The calculations make only limited use of reaction models and assumptions; they use the energy spectra observed for the particles of interest in the detectors of interest [4]. This minimizes the effect of errors in the energy calibrations as well as items such as the emitter velocity, its temperature, etc.

An outline of the steps in the calculation is as follows. (a) Convert observed ejectile spectra from laboratory to an assumed emitter frame (EF). (b) Include emitter recoil effect with an assumed emitter mass to obtain channel energy spectra. (c) Choose a channel energy  $E_i$  for the ejectile (or particle) and its direction from a zone larger than that of the EMRIC array. (d) Calculate the asymptotic particle direction in the EF. (e) Select exit channel angular momentum or  $\ell_i$  values at random from a triangular distribution and direct them at random in the plane perpendicular to the particle direction. (f) Given a velocity and radius of the emitting source, these choices of  $E_i$  and  $\ell_i$  allow one to define the initial position and momentum of the  $i$ th ejectile at the surface of the emitting source. (g) After emission of the first

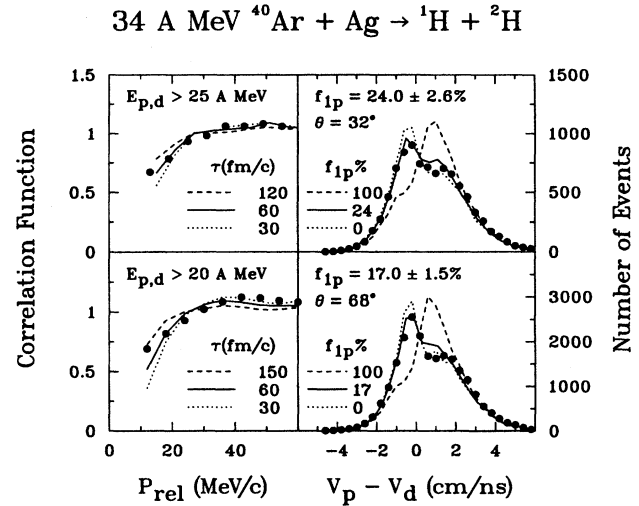


FIG. 2. Similar to Fig. 1 but for  ${}^1\text{H}$ - ${}^2\text{H}$  pairs. The calculated curves for the velocity difference spectra use the best-fit values of  $\tau$  from the left panel and then vary the fraction  $f_{1p}$  for proton emission first.

particle, a time  $t$  is selected for emission of the second particle; this choice is made from the assumption of exponential decay  $P(t) = \exp(-t/\tau)$  with a given input value of the mean lifetime  $\tau$ . A three-body trajectory is then calculated and filtered by the experimental acceptance [3]. (For this reaction we find that three-body trajectories give essentially the same results as many-body trajectories.)

Calculations are shown in Fig. 1 for each pair of plots with the input  $\tau$  values as indicated on the left. From the best overall fit a mean lifetime  $\tau_d$  was assigned; by similar analyses values of  $\tau_i$  were determined with data for  ${}^3\text{H}$ - ${}^3\text{H}$  pairs. The values of  $\tau_d$  and  $\tau_i$  vary strongly with ejectile velocity; they will be discussed below along with Fig. 4. In separate calculations the roles of various assumed input quantities were explored. We used an emitter velocity from the average for heavy residual nuclei reported in Ref. [1], but changes of even 50% do not affect the calculated results. Initial emitter mass numbers  $A_i$  were taken from [1,10] and normal nuclear radii were used to assign the initial distance between emitter and ejectile. Reduction of  $\sim 30\%$  in  $A_i$  has only a small effect on the calculated curves. Use of a smaller nuclear density (i.e., an expanded source) would lead to somewhat smaller assignments for  $\tau$ ; therefore, these  $\tau$  values can be taken as upper limits for cases of  $\tau \leq 100 \text{ fm/c}$  [11].

For like-particle pairs, as in Fig. 1, we use primarily the  $P_{\text{rel}}$  correlation functions to obtain  $\tau$ ; the velocity difference spectra provide useful confirmation by their agreement. For unlike particle pairs, however, these velocity difference spectra add an independent constraint on the emission order [4,7,9]. In Fig. 2 we illustrate this with  ${}^1\text{H}$ - ${}^2\text{H}$  pairs, each selected by a high velocity cut as indicated. The  $P_{\text{rel}}$  correlation function is sensitive to the  $\tau$  value [e.g., 3]; but it is essentially insensitive to the fraction  $f_{1p}$  for proton emission first. The velocity difference spectra for unlike particles are generally asymmetric about  $V_p - V_d = 0$ ; this asymmetry is related to differences in the individual particle velocity spectra, but it is also driven by the emission order. Shown for comparison are curves calculated with  $f_{1p} = 0$  and 100%. In

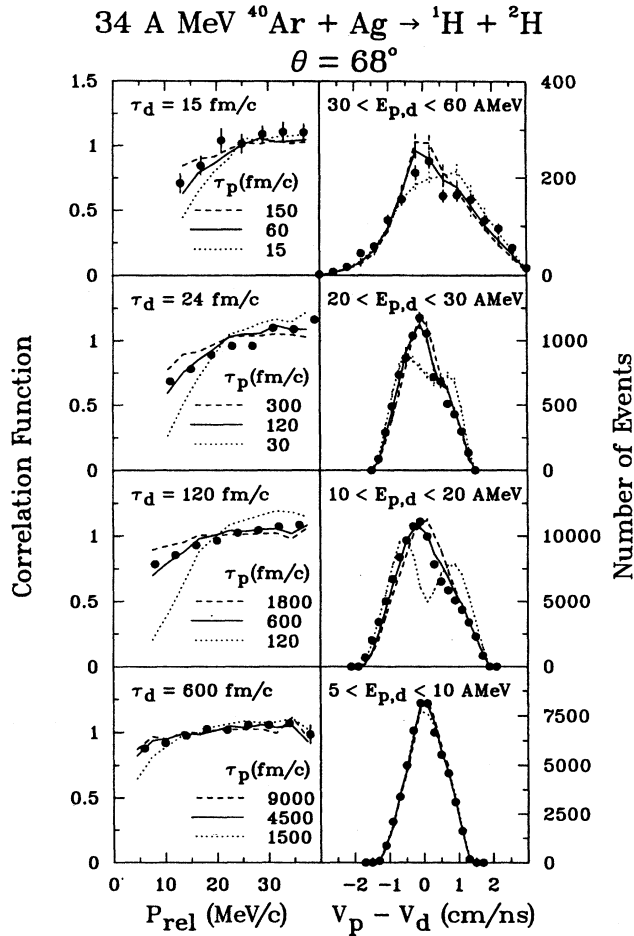


FIG. 3. Similar to Figs. 1 and 2 for  $^1\text{H}$ - $^2\text{H}$  pairs but with a different approach to the calculated curves. Values of  $\tau_d$  (as indicated on the left) were taken from the systematics (see Fig. 1); then several calculated curves are obtained for various values of  $\tau_p$  as indicated. Velocity cuts for each  $^1\text{H}$  and  $^2\text{H}$  were applied as indicated on the right.

short there is high detection efficiency for pairs if the higher velocity particle is emitted first and the contrary. The data in Fig. 2 show a high peak for  $V_d > V_p$  compared to only a shoulder for  $V_p > V_d$ . This indicates that deuterons predominate as the first particle emitted for this velocity cut. Least squares fits to these asymmetric velocity difference spectra lead to the low values indicated ( $f_{1p} = 24$  or  $17\%$ ) for proton emission prior to the deuterons for the conditions indicated. The use of a correlation function in  $V_p - V_d$  leads to identical conclusions, but its shape does not lead to an intuitive interpretation.

Figure 3 illustrates a more interesting way to analyze such data, one that seeks to characterize the  $^1\text{H}$  and  $^2\text{H}$  emission processes in terms of two separate exponential decays with their respective mean lifetimes  $\tau_p$  and  $\tau_d$ . Such a characterization will generate a specific average emission order and time intervals between ejectiles as a direct result of the relative magnitudes of these lifetimes. From Fig. 1 for  $^2\text{H}$ - $^2\text{H}$  pairs we have determined  $\tau_d$  values for several velocity (or energy) cuts. For the analysis in Fig. 3 we have used these values of  $\tau_d$  from the  $^2\text{H}$ - $^2\text{H}$  data (as indicated) and then

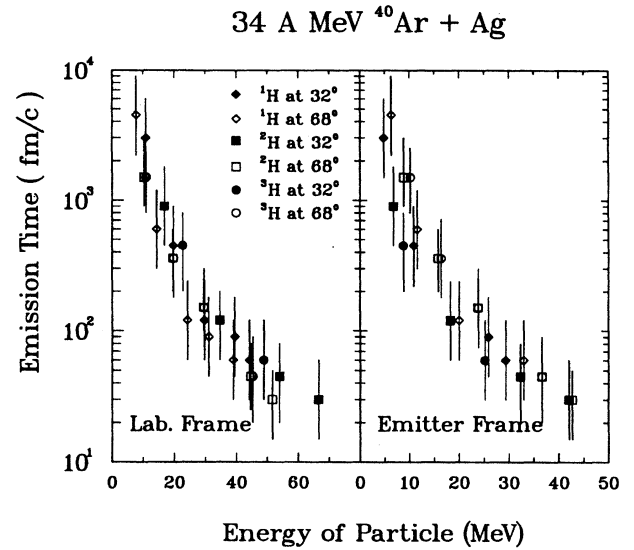


FIG. 4. Summary graph for lifetimes of each ejectile obtained at  $32^\circ$  and  $68^\circ$ . The abscissa is the average laboratory energy in (a) and the average emitter-frame energy in (b). The average emitter-frame velocity used here and in Fig. 5 was taken from data in Ref. [1].

have varied only the value of  $\tau_p$  to get best fits to the combinations of correlation functions and velocity difference spectra at  $\theta_{\text{lab}} = 68^\circ$ . Calculated curves are shown for four ejectile velocity intervals, each with several values of  $\tau_p$  as indicated. The best-fit lifetimes vary enormously, from  $\sim 4500$  fm/c to  $\sim 60$  fm/c as the velocity increases. This series of analyses has also been performed for ejectile pairs observed with EMRIC centered at  $32^\circ$ .

Figure 4 shows the complete set of mean lifetime values as a function of average ejectile energy as observed in the laboratory and as transformed into the emitter frame. As a consistency test of this pattern we have compared the data shown in Fig. 2 to simulations that use the results given in Fig. 4. For each selected energy of  $^1\text{H}$  or  $^2\text{H}$  one chooses the  $\tau$  value from Fig. 4; thus there are no free parameters. The calculated curves account for the data in an acceptable way with  $f_{1p}$  values of 26% and 33% for  $69^\circ$  and  $32^\circ$ , respectively. These results indicate a reasonable overall consistency in the approach. We have avoided the use of  $^1\text{H}$ - $^1\text{H}$  correlations here due to the possible ejection of small amounts of preformed  $^2\text{He}$ , which would greatly complicate their interpretation [11]. In addition, this interwoven use of data for  $^1\text{H}$ ,  $^2\text{H}$ , and  $^3\text{H}$  gives a broad view of the reaction pathways, which goes well beyond that from  $^1\text{H}$ - $^1\text{H}$  as deduced elsewhere [12], e.g.

It is very surprising that these different ejectiles exhibit such similar behavior over such a wide range of energy and lifetime and for both  $32^\circ$  and  $68^\circ$ , because one would expect the mechanisms to be very different. The energy spectra in Fig. 5 illustrate this point. They show a variation with angle, which can be mainly accounted for by evaporation from a single emitter for back angles (e.g., for  $\theta > 68^\circ$ ) [1,2,6,7]. However, for  $\theta = 32^\circ$  the observed spectrum has a completely different shape from that calculated for evaporation from the same source. The spectral shapes imply that  $^2\text{H}$  and

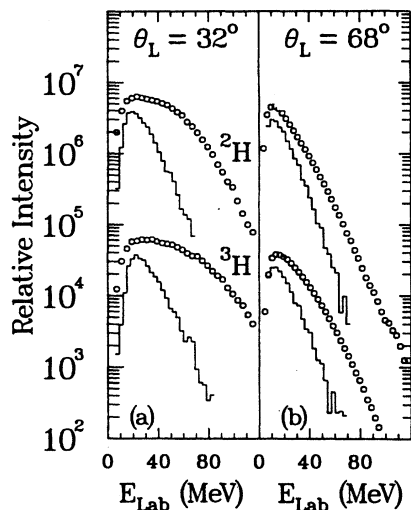


FIG. 5. Energy spectra for  $^2\text{H}$  and  $^3\text{H}$  compared to evaporation model calculations [13,14] for an emitter with average linear momentum transfer of 85% [1,7]. For our trajectory calculations we use the observed energy spectra to start, and a program test of steps (a-f) is the simulation's rematch to these spectra.

$^3\text{H}$  at  $32^\circ$  arise from additional mechanisms, e.g., prethermalization emissions. Our expectation was that such a mixture of mechanisms at  $32^\circ$  would lead to a different pattern of  $\tau$  values when compared to that for an evaporationlike source that seems to dominate the  $68^\circ$  spectrum.

One possible rationalization of this behavior can be sought by considering the time interval that is required for fusion. Schematically, this time can be said to be approximately the nuclear radius divided by the projectile velocity, i.e.,  $\sim 50 \text{ fm}/c$ . Direct emission, such as that calculated in molecular dynamics models [15], e.g., is indeed predicted to occur on just such a time scale. Emission after fusion and complete thermalization must, therefore, come later in the collision sequence. Figure 4 shows that the observed  $\tau$  values reach  $\sim 30 \text{ fm}/c$  for the highest ejectile energies at both  $32^\circ$  and  $68^\circ$ . Thus one might conclude that these very short

ejectile emission times are being limited as they approach  $\sim 50 \text{ fm}/c$  by dynamical constraints demanded by the time required for the interpenetration of projectile and target nuclei. Much longer emission times for the lower energy particles seem to reflect an extensive internuclear collision cascade required for thermalization. The occurrence of such a broad span of particle emission times (and presumably emitters) may well be a critical feature that has clouded the interpretation of  $^1\text{H}$ - $^1\text{H}$  correlations [16–18], e.g. In the absence of velocity cuts the apparent space time extent of the source would include averaging over an enormously complicated set of emitters.

Our qualitative conclusion is that the higher energy ejectiles at both  $32^\circ$  and  $68^\circ$  come from prethermalization emission in contrast to the lower energy ejectiles that are emitted after much more extensive thermalization. Therefore, the use of the phrase “projectilelike source” or “intermediate rapidity source” (in the context of the high energy  $^{1,2,3}\text{H}$  from this reaction) should be taken to include ejectiles, which retain some memory of the translational motion of the projectile, but are almost directly ejected from the collision zone. This notion of “source” is quite different from that of a heated projectilelike fragment which exits from the collision zone and then suffers evaporationlike decay. The latter process is almost surely important for peripheral collisions but is much less important for the central collisions studied here [1,2]. This work shows that LCP emission from the central collision zone covers the full dynamic range of reaction times, from essentially direct ejection to extremely slow particle evaporation. This wide range of processes makes it very difficult to use an energy integrated set of LCP data to probe the space-time extent of the reaction zone. The fast, high velocity particles, however, are of particular interest since they can provide just such a probe; in addition they offer a very interesting possibility analogous to a start signal for a stopwatch on the reaction dynamics [9,15].

Financial support has been provided in part by the U.S. Department of Energy and by the CNRS of France. M.E.B. and A.M.R. acknowledge partial support from CONACYT, Grant No. 3173E.

- [1] M. T. Magda and J. M. Alexander, in *Topics in Atomic and Nuclear Collisions*, edited by B. Remaud (Plenum, New York, 1994), pp. 97–121; M. T. Magda, E. Bauge, A. Elmaani, T. Braunstein, C. J. Gelderloos, N. N. Ajitanand, J. M. Alexander, T. Ethvignot, P. Bier, L. Kowalski, P. Désesquelles, H. Elhage, A. Giorni, S. Kox, A. Lleres, F. Merchez, C. Morand, P. Stassi, J. B. Benrachi, B. Chambon, B. Cheynis, D. Drain, and C. Pastor, *Phys. Rev. C* (to be submitted).
- [2] T. Ethvignot, A. Elmaani, N. N. Ajitanand, J. M. Alexander, E. Bauge, P. Bier, L. Kowalski, M. T. Magda, P. Désesquelles, H. Elhage, A. Giorni, D. Heuer, S. Kox, A. Lleres, F. Merchez, C. Morand, D. Rebreyend, P. Stassi, J. B. Viano, S. Benrachi, B. Chambon, B. Cheynis, D. Drain, and C. Pastor, *Phys. Rev. C* **43**, R2035 (1991).
- [3] A. Elmaani, N. N. Ajitanand, T. Ethvignot, and J. M. Alexander, *Nucl. Instrum. Methods Phys. Res. Sect. A* **313**, 401 (1992).
- [4] C. J. Gelderloos and J. M. Alexander, *Nucl. Instrum. Methods Phys. Res. Sect. A* **349**, 618 (1994).
- [5] F. Merchez, S. Kox, C. Perrin, J. Mistretta, J. C. Gondrand, and L. N. Imouk, *Nucl. Instrum. Methods Phys. Res. Sect. A* **275**, 133 (1989).
- [6] A. Elmaani, J. M. Alexander, N. N. Ajitanand, R. A. Lacey, S. Kox, E. Liatard, F. Merchez, T. Motobayashi, B. Noren, C. Perrin, D. Rebreyend, Tsan Ung Chan, G. Auger, and S. Groult, *Phys. Rev. C* **49**, 284 (1994); A. Elmaani and J. M. Alexander, *ibid.* **47**, 1321 (1993).
- [7] C. J. Gelderloos, Ph.D. thesis, Department of Physics, SUNY at Stony Brook, New York, 1994.
- [8] M. T. Magda, T. Ethvignot, A. Elmaani, J. M. Alexander, P. Désesquelles, H. Elhage, A. Giorni, D. Heuer, S. Kox, F. Merchez, C. Morand, D. Rebreyend, P. Stassi, J. B. Viano, S. Benrachi, B. Chambon, B. Cheynis, D. Drain, and C. Pastor, *Phys. Rev. C* **45**, 1209 (1992).

- [9] C. J. Gelderloos, J. M. Alexander, N. N. Ajitanand, E. Bauge, A. Elmaani, T. Ethvignot, L. Kowalski, R. A. Lacey, M. E. Brandan, A. Giorni, D. Heuer, S. Kox, A. Lleres, A. Menchaca-Rocha, F. Merchez, D. Rebreyend, J. B. Viano, B. Chambon, B. Cheynis, D. Drain, and C. Pastor, *Phys. Rev. Lett.* **75**, 3082 (1995).
- [10] T. Ethvignot, N. N. Ajitanand, J. M. Alexander, A. Elmaani, C. J. Gelderloos, P. Désesquelles, H. Elhage, A. Giorni, D. Heuer, S. Kox, A. Lleres, F. Merchez, C. Morand, D. Rebreyend, P. Stassi, J. B. Viano, F. Benrachi, B. Chambon, B. Cheynis, D. Drain, and C. Pastor, *Phys. Rev. C* **47**, 2099 (1993).
- [11] J. M. Alexander, A. Elmaani, L. Kowalski, N. N. Ajitanand, and C. J. Gelderloos, *Phys. Rev. C* **48**, 2874 (1993).
- [12] M. A. Lisa, C. K. Gelbke, P. Decowski, W. G. Gong, E. Gualtieri, S. Hannuschke, R. Lacey, T. Li, W. G. Lynch, G. F. Peaslee, S. Pratt, T. Reposeur, A. M. Vander Molen, G. D. Westfall, J. Yee, and S. Yennello, *Phys. Rev. Lett.* **71**, 2863 (1993).
- [13] N. N. Ajitanand and J. M. Alexander, "MODGAN: A Modular Nuclear Evaporation Code Based On The Weighted Monte Carlo Technique," Stony Brook report, 1995 (unpublished).
- [14] S. Shlomo, *Nucl. Phys.* **A539**, 17 (1992).
- [15] J. P. Bondorf, A. S. Botvia, I. N. Mishustin, and S. R. Souza, *Phys. Rev. Lett.* **73**, 628 (1994).
- [16] G. J. Kunde, J. Pochodzalla, E. Berdermann, B. Berthier, C. Cerruti, C. K. Gelbke, J. Hubele, P. Kreutz, S. Leray, R. Lucas, U. Lynen, U. Milkau, C. Ngo, C. H. Pinkenburg, G. Raciti, H. Sann, and W. Trautmann, *Phys. Rev. Lett.* **70**, 2545 (1993).
- [17] D. Rebreyend, F. Merchez, B. Noren, E. Andersen, M. Cronqvist, J. C. Gondrand, H. A. Gustafsson, B. Jager, B. Jakobsson, B. Khelfaoui, S. Kox, A. Kristiansson, G. Lovhoiden, S. Mattsson, J. Mistretta, A. Oskarsson, C. Perrin, M. Rydehell, O. Skeppstedt, T. F. Thorsteinsen, M. Westenius, and L. Westerbergh, *Phys. Rev. C* **46**, 2387 (1992).
- [18] D. A. Cebra, W. Benenson, Y. Chen, E. Kashy, A. Pradham, A. Vander Molen, G. D. Westfall, W. K. Wilson, D. J. Morissey, R. S. Tickle, R. Korteling, and R. L. Helmer, *Phys. Lett. B* **277**, 336 (1989).